New COX-2/5-LOX Inhibitors: Apoptosis-Inducing Agents Potentially Useful in Prostate Cancer Chemotherapy

Nicole Pommery,[†] Thierry Taverne,[†] Aurélie Telliez,[†] Laurence Goossens,[†] Caroline Charlier,[‡] Jean Pommery,[†] Jean-François Goossens,[†] Raymond Houssin,[†] François Durant,[‡] and Jean-Pierre Hénichart*[,†]

Institut de Chimie Pharmaceutique Albert Lespagnol, EA 2692, Université de Lille 2, BP 83, 59006 Lille, France, and Laboratoire de Chimie Moléculaire Structurale, Facultés Universitaires Notre-Dame de la Paix, rue de Bruxelles, 5000 Namur, Belgium

Received January 19, 2004

The arachidonic acid metabolizing enzymes cyclooxygenase-2 (COX-2) and lipoxygenases (LOXs) have been found to be implicated in a variety of cancers, including prostate cancer. To develop new therapeutic treatments, it therefore seemed interesting to design dual COX-2/5-LOX inhibitors. We report here the synthesis and in vitro pharmacological properties of diarylpyrazole derivatives that have in their structure key pharmacophoric elements to obtain optimal interaction with subsites of active pockets in both enzyme systems. Using a molecular modeling approach, a set of SAR data is proposed, highlighting the importance of the sulfonyl group of one of the aryl moieties in terms of proliferation inhibition and/or apoptosis induction.

Introduction

New studies on relationships between polyunsaturated fatty acid metabolism and carcinogenesis have led to the identification of new molecular targets in cancer chemoprevention research. These targets include arachidonic acid metabolizing enzymes such as cyclooxygenases (COXs) and lipoxygenases (LOXs), which lead to the formation of various eicosanoids involved in a variety of human diseases, such as inflammation, fever, arthritis, and, more recently discovered, cancer.[1−4]

The implications of COXs and LOXs have been discussed in numerous types of cancers, including colon, pancreas, breast, lung, skin, urinary bladder, or liver cancers, but inhibiting these enzymes seems to be even more promising to halt or reverse the progression of prostate cancer.[5] In fact, because of the unavailability of effective systemic therapies, this cancer is usually fatal once the tumor cells invade the outer area of the gland. Recent data has demonstrated the involvement of COX-2 in both in vitro proliferation and in vivo tumor growth rate.[6−9] Other works have highlighted the role played by COX-2 in disturbing the balance between matrix metalloproteinases (MMPs) and the tissue inhibitors of metalloproteinases (TIMPs) in prostate cancer cells, indicating the potential use of COX inhibitors in the prevention and therapy of prostate cancer invasion.[10] Moreover, dynamically evolving research shows the different roles of LOXs and their metabolic products in carcinogenesis and chemoprevention.[11] A more detailed understanding of mechanisms is needed, but data suggests that one group of LOXs, including 5-, 8- and 12-LOX, has procarcinogenic roles,[11,12] while 15-LOX metabolites have the opposite effect on the growth of prostatic adenocarcinoma cells.[13] 15-Hydroxyeicosatetraenoic acid (15-HETE), produced by 15-LOX-2, activates peroxisome proliferator-activated receptor γ (PPARγ) and inhibits proliferation,[14] whereas (13*S*)-hydroxyoctadecadienoic acid, (13*S*)-HODE, the 15-LOX-1 metabolite, is reported to up-regulate the MAP kinase signaling pathway and then down-regulate PPARγ and increase tumorigenesis of the human prostate cancer cell line.[15]

Chart 1

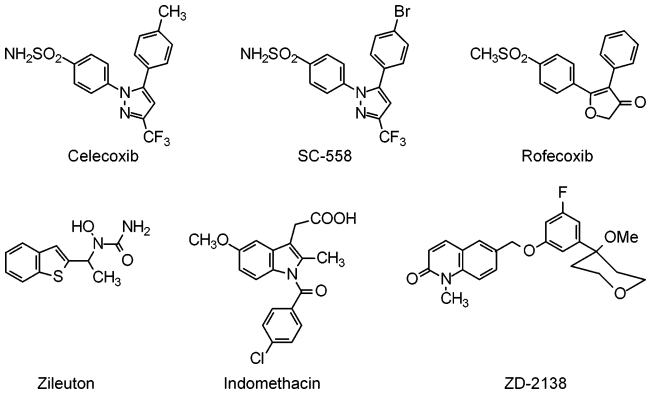

Many compounds widely used in the treatment of pain and inflammation, such as celecoxib, rofecoxib, zileuton, and indomethacin (Chart 1), have been tested in vitro and in vivo on cell growth and non-necrotic cell death.[16−19] However, the signaling mechanism used by COX-2/LOXs inhibitors to mediate apoptotic death in cancer cells remains the focus of many investigations, and there is increasing evidence to suggest that COX-2 inhibition may have no role in NSAID-mediated apoptotic cell death.[18,20] Some findings suggest that the apoptosis-inducing effects and antiangiogenic activity of celecoxib may be partly attributable to a COX-2-independent pathway,[19,21] and the structural requirements for the induction of apoptosis in prostate cells seem different from those for COX-2 inhibition.

Over and above, to develop new therapeutic treatments, it seems in any case interesting to design dual COX-2/LOX inhibitors, first to prevent a drift of arachi-

* To whom correspondence should be addressed. Phone: +33-3-2096-4374. Fax: +33-3-2096-4906. E-mail: henicha@pharma.univ-lille2.fr.
[†] Université de Lille 2.
[‡] Facultés Universitaires Notre-Dame de la Paix.

10.1021/jm0407761 CCC: $27.50
Published on Web 10/30/2004

Scheme 1[a]

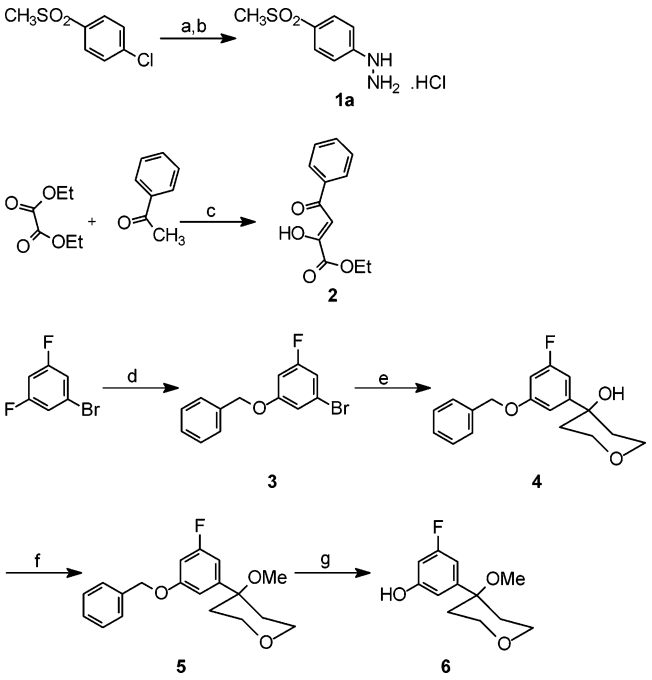

[a] Reagents and conditions: (a) $NH_2NH_2 \cdot H_2O$, EtOH, 160 °C, 1 h; (b) 37% HCl, EtOH, 0.5 h; (c) EtONa, EtOH, reflux, 2 h; (d) NaH, $C_6H_5CH_2OH$, DMA, 4 °C to rt, 20 h; (e) *n*-BuLi, 3,4,5,6-tetrahydro-4*H*-pyran-4-one, THF, −78 °C, 4 h; (f) NaH, CH_3I, DMF, 4 °C to rt, 3 h; (g) 20% $Pd(OH)_2$, EtOH, rt, 15 h.

donic acid metabolism toward the other pathway, which would lead to potential side effects, and second to force cell death, that is, to kill specific cells possessing a high flux of arachidonic acid and its metabolites in prostate and colon cancer cells.[22]

We have recently reported the excellent properties of a dual molecule as regards both in vitro/in vivo COX-2 and 5-LOX inhibition.[23] We describe here the synthesis and biological properties of new diarylpyrazoles structurally related to this lead compound. The emphasis will be focused on structure−function relationships with a view to delineating the influence of key COX/LOX pharmacophoric groups on cell proliferation inhibition and/or apoptosis induction.

Results and Discussion

Chemistry. Arylhydrazines **1b**−**j** were commercially available, whereas methanesulfonylhydrazine **1a** was obtained (Scheme 1) by nucleophilic substitution of 4-chlorophenylmethyl sulfone with hydrazine. β-Diketone **2** was prepared (Scheme 1) by Claisen reaction between acetophenone and diethyl oxalate, and phenol **6** was synthesized by a reaction sequence adapted from a published procedure.[24]

The synthesis of 1,5-diarylpyrazoles **7a**−**j** was done (Scheme 2) by regioselective cyclization of arylhydrazines **1a**−**j** with β-diketone **2** in refluxing ethanol.

Esters **7a-j** were reduced with $LiBH_4$ (anhydrous THF, argon), yielding the primary alcohols **8a**−**j**. Bromination of the crude products with $(C_6H_5)_3P$−NBS gave the pyrazoles **9a**−**j**, which were sufficiently stable to be readily purified by short silica gel flash chromatography.[25] The alkyl bromides were reacted with phenol **6** (Cs_2CO_3/DMF, 90 °C) to yield the diphenylpyrazoles **10a**−**j**. 3-Phenoxymethylpyrazoles **10k**−**m** were obtained by reacting substituted fluorobenzenes with the sodium salt of pyrazole **8a** prepared in situ (NaH, DMA, 20 °C), whereas ethers **10n**−**s** were obtained from the reaction of pyrazole **9a** with diverse phenols (Cs_2CO_3/DMF, 90 °C).

Biological Data. Inhibition of COX-2 and 5-LOX Activities. Compounds **10a**−**s** were first tested for their ability to inhibit COX-2 and 5-LOX activities (Table 1).

Scheme 2[a]

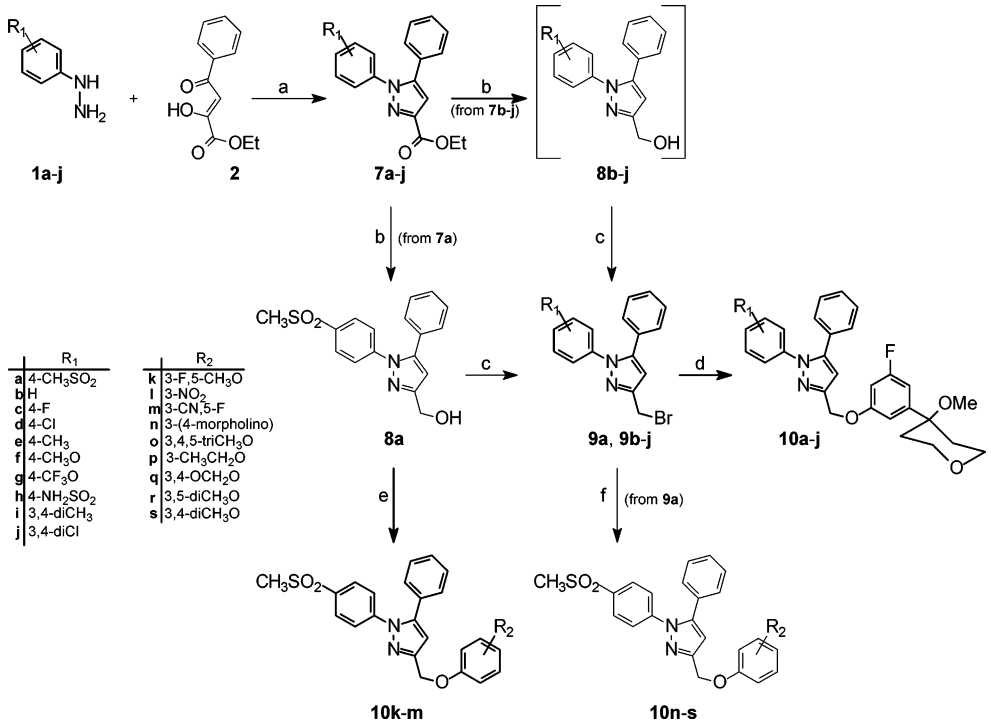

[a] Reagents and conditions: (a) EtOH, reflux, 3 h; (b) $LiBH_4$, THF, rt, 72 h; (c) $(C_6H_5)_3P$, NBS, CH_2Cl_2, rt, 15 h; (d) **6**, Cs_2CO_3, DMF, 90 °C, 1 h; (e) NaH, F−Ar−R_2, DMA, 0 °C to 20 °C, 15 h; (f) HO−Ar−R_2, Cs_2CO_3, DMF, 90 °C, 1 h.

Table 1. Enzymatic Activities for Compounds **10a**−**s**

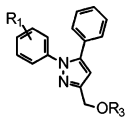

compd	R_1	R_3	IC_{50} (μM)[a] COX-1[b]	COX-2[b]	5-LOX[c]	selectivity COX-1/COX-2
celecoxib			13.5	0.036	> 10	375
ZD-2138			> 100	> 100	0.083	-
10a	4-CH_3SO_2	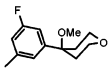	26.08	0.045	0.30	579
10b	4-H	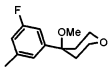	7.14	0.61	0.57	12
10c	4-F	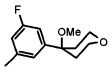	1.13	0.96	0.48	1
10d	4-Cl	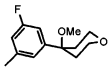	1.81	0.93	0.83	2
10e	4-CH_3	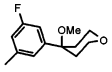	1.56	0.93	0.72	1
10f	4-CH_3O	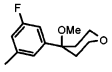	0.036	0.30	0.77	< 1
10g	4-CF_3O	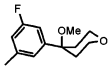	nd[d]	0.82	0.85	-
10h	4-NH_2SO_2	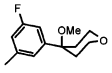	25.7	0.10	0.74	257
10i	4,5-diCH_3	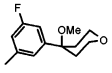	nd[d]	0.41	0.76	-
10j	4,5-diCl	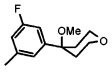	nd[d]	0.70	0.80	-
10k	4-CH_3SO_2		44.33	0.31	> 10	142
10l	4-CH_3SO_2		> 100	0.74	> 10	> 134
10m	4-CH_3SO_2		99.56	0.57	> 10	176
10n	4-CH_3SO_2	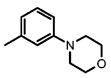	38.08	0.92	> 10	41
10o	4-CH_3SO_2		17.59	0.22	> 10	78
10p	4-CH_3SO_2		> 100	0.90	> 10	> 112
10q	4-CH_3SO_2		15.81	0.45	> 10	35
10r	4-CH_3SO_2		25.05	0.87	> 10	29
10s	4-CH_3SO_2		> 100	0.70	> 10	> 142

[a] Values correspond to $n = 2$. [b] Inhibition produced by tested compounds on CHO transfected cell PGE_2 production. [c] Inhibition of 5-HETE generation from human whole blood. [d] nd = not determined.

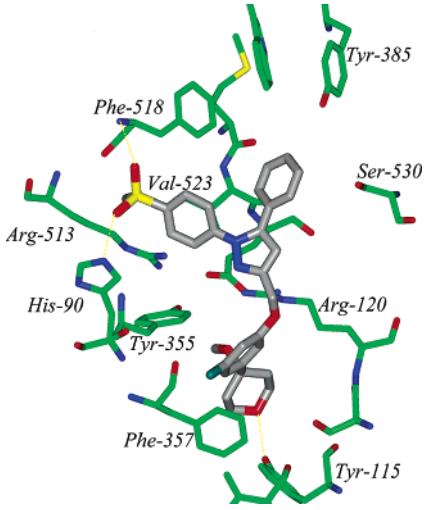

Figure 1. Docking of **10a** into the COX-2 active site. Different regions of the active site as well as key residues are explicitly shown. Yellow dotted lines represent H bonds.

For this purpose, inhibition of PGE_2 biosynthesis was evaluated by immunoassay in COX-1 and COX-2 transfected CHO cells. On the other hand, HPLC analysis of calcium ionophore A-stimulated 5-HETE production made assessment of 5-LOX activity in human whole blood samples possible. In our models, compound **10a**, a combination of standard diaryl heterocyclic methyl sulfone—such as the COX-2 part—and the 4-methoxytetrahydropyran structural part of ZD-2138—a selective 5-LOX inhibitor (Chart 1)—was the most potent inhibitor of the whole series. It showed IC_{50} values of 45 nM and 0.3 μM, respectively, for COX-2 and 5-LOX inhibition and showed valid COX-1/COX-2 selectivity.

Replacement of the 4-methoxytetrahydropyran group of **10a** by electron-donor and electron-withdrawing groups (**10k**−**s**) produced a complete loss of LOX inhibition.

Replacement of the methanesulfonyl moiety by various groups (**10b**−**j**) reduced PGE_2 synthesis inhibition from transfected CHO cells. Only **10h**, which presents an aminosulfonyl substituent (celecoxib-like), demonstrated a comparable inhibitory profile toward COX-2. This confirms that both methanesulfonyl and aminosulfonyl moieties are important for optimal COX-2 inhibition.[26]

Docking in Human COX-2 and 5-LOX Models. High-resolution structural information on COX−inhibitor complexes led to a detailed description of the COX active site.[27] This consists of a long narrow hydrophobic channel extending from the membrane-binding domain (the lobby) to the heme cofactor. Despite their similarity, the COX-2 active site is about 20% larger and has a slightly different form from that of COX-1. The change of two isoleucines (Ile-434 and Ile-523) in COX-1 by two valines in COX-2 opens up an extra hydrophilic nook off the main channel, appreciably increasing the volume of the COX-2 active site. Another essential amino acid difference consists of Arg-513 inside this side pocket, in place of a histidine in COX-1. It generates a specific interaction site for inhibitors in COX-2.

Two different binding modes can be considered among the inhibitors studied (**10a**−**j**). The first (Figure 1), "coxib-like", is close to that adopted by SC-558 (Chart 1) cocrystallized with COX-2 (PDB entry 6COX).[28] The substituted aryl ring inserts into the side pocket and the other phenyl group occupies the upper part of the channel. The additional 5-LOX pharmacophoric group fills a hydrophobic cavity at the mouth of the active site. This was the most favorable interaction hypothesis proposed by *GOLD* for five of the 10 dual inhibitors, i.e., **10a**, **10d**−**10f**, and **10h**. All these compounds share three important interaction points (Tyr-355, Arg-120 and Phe-518) as well as one hydrogen bond that involves tetrahydropyran oxygen with Tyr-115. However, in contrast to the other substituents, methanesulfonyl and aminosulfonyl moieties (**10a** and **10h**) form two other H bonds, with His-90 and the backbone of Phe-518, increasing the stability of the complexes (ΔE ranging from −3.6 to −5.4 kcal mol^{-1}). These interactions appear to play a key role in the optimal inhibition of the enzyme.

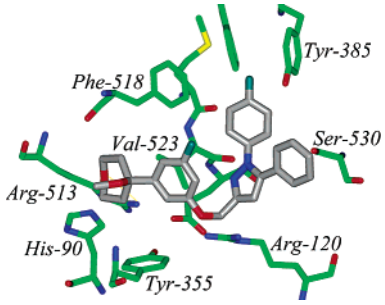

Figure 2. Docking of **10c** inside the COX-2 active site as an illustration of the second binding mode. Yellow dotted lines represent H bonds.

The second binding mode, adopted by **10b**, **10c**, **10g**, **10i**, and **10j**, inserts the 5-LOX fragment into the hydrophilic side pocket (Figure 2), while the diaryl heterocycle, characteristic of COX-2 inhibitors, is constrained in the hydrophobic channel. Whereas two interactions through XH-π contact (X = O or C) with Ser-530 and Val-523 can uniformly be observed among the five inhibitors, they show diverse interaction patterns with the active site residues. On one hand, compounds **10b**, **10c**, and **10g** form an H-bond involving Arg-513 and, on the other hand, **10i** and **10j** interact through a weak H-bond with His-90 and Phe-518, respectively. However, despite these interactions, the lesser stability of these complexes, in comparison to that of **10a** and **10h** in COX-2, can be assessed by the smaller global interaction energy (ΔE ranging from 7.6 to 10.7 kcal mol^{-1}).

Another mode of interaction for **10a** and **10h** inside the COX-2 active site was also proposed by GOLD, i.e., the polar moiety (methanesulfonyl and aminosulfonyl functions) lying in the proximity of Tyr-385 and Ser-530. This was similar to a new inverted orientation, recently revealed by the crystallographic structure of diclofenac bound to COX-2.[29] Its carboxylic acid moiety, in contrast to other NSAIDs, is situated in the upper part of the channel, interacting through H-bonds with Tyr-385 and Ser-530. However, the resulting **10a**− or **10h**−COX-2 complexes were much less stable than the "coxib-like" ones (ΔE ranging from 7.3 to 8.1 kcal mol^{-1}).

In contrast to COX enzymes, structural knowledge about the 5-LOX active site is much more limited. It was therefore first explored with different GRID probes,[30]

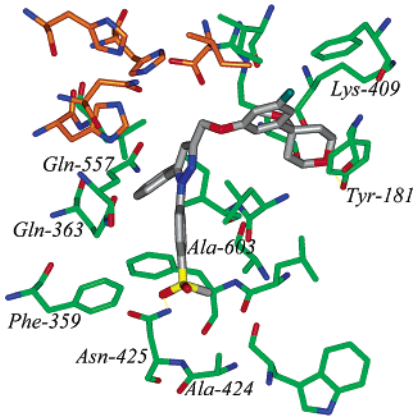

Figure 3. Docking of **10a** inside the 5-LOX active site. Key residues are explicitly shown and the iron−ligand residues are colored orange. Yellow dotted lines represent H bonds.

characteristic of inhibitors, to identify potential interaction regions and to support their most likely binding mode(s). The active site is a deep cleft, bent in shape, that includes the catalytic non-heme iron and a positively charged residue (Lys-409) at its entrance. It appears to be preponderantly hydrophobic in nature with some polar residues.

The binding mode proposed for **10a** is shown in Figure 3. It inserts the "COX fragment" deep in the cavity with the methanesulfonyl moiety at the bottom, interacting through a H-bond with Asn-425. The "5-LOX part" fills the entrance of the active site and also forms an H-bond with the tetrahydropyran oxygen and Tyr-181.

The other compounds bind to 5-LOX in the same way as **10a**. However, only **10h** can interact with Asn-425, meaning that complexes are less stable (ΔE ranging from 3.2 to 6.2 kcal mol^{-1}). This modeling study seems to be insufficient to understand the lower 5-LOX inhibitory activity of **10h** vs **10a**, as the global interaction energy between the two complexes is very small (ΔE = 0.9 kcal mol^{-1}).

While the importance of methanesulfonyl and aminosulfonyl moieties has been established in COX-2 inhibition, further SAR could help in understanding and validating the proposed interaction pattern with 5-LOX.

Cellular Activity. The antiproliferative activity of compounds **10a**−**j** was evaluated against two human prostate carcinoma cell lines, the LNCaP and PC 3 lines, respectively androgen-sensitive and androgen-independent cells (Table 2). Assays with celecoxib and rofecoxib as reference compounds were included for comparison. Most tested compounds showed no effect on cell growth up to the concentration of 100 μM. Growth inhibitory potency was relatively weak for **10i** and **10j**, but an interesting activity was observed with **10a** and **10h**, bearing aminosulfonyl and methanesulfonyl groups. Compounds **10a**, **10h**, and celecoxib showed antiproliferative activities ranging between 50 and 100 μM. When compared with **10a**, **10h** exhibited higher potency on the invasive PC 3 cell line, usually described as resistant to current chemotherapeutics. We also observed that compound **10h** only caused inhibition of MMP-9 secretion induced by PC 3 cells (zymographic data not shown). This decrease in a key enzyme of extracellular matrix proteolysis during invasion shows the potentially extensive interest of **10h**, not only in the proliferative phase but also in the metastatic process sustaining prostate cancer evolution.

Table 2. Activity of Compounds 10**a**−**j** on the Proliferation of LNCaP and PC 3 Cancer Cell Lines[a]

	IC_{50} (μM)[b] or % inhibition[c]	
compd	LNCaP	PC 3
celecoxib	50.4 ± 6.3	47.0 ± 4.6
rofecoxib	0%	15%
10a	83.4 ± 8.7	45%
10b	0%	0%
10c	3%	7%
10d	0%	0%
10e	18%	0%
10f	nd	nd
10g	0%	0%
10h	49.7 ± 4.5	45.9 ± 2.6
10i	26%	55.0 ± 3.7
10j	32%	21%

[a] Activity determined with the MTT method. [b] Mean from at least four independent determinations. [c] Compounds tested at the concentration of 100 μM.

Table 3. Inhibitory Effect of Compounds 10**a**−**j** (10 μM) on the Progression of LNCaP Cells in the Cellular Cycle[a]

	Cell population in cycle phases (%)			
compd	Sub-G1	G1	S	G2-M
untreated control	4.2	69.1	11.6	15.2
celecoxib	3.9	75.7	9.0	11.3
rofecoxib	4.0	69.4	11.4	15.2
10a	3.6	70.1	11.2	14.7
10b	3.0	72.9	10.6	13.9
10c	4.0	71.3	9.7	15.3
10d	2.5	75.5	11.1	11.1
10e	3.5	71.3	10.7	14.6
10f	2.8	69.0	11.4	17.0
10g	3.6	74.7	10.6	11.0
10h	10.8	74.2	6.9	8.2
10i	3.9	69.5	11.5	15.0
10j	4.6	68.2	11.5	15.5

[a] Flow cytometric cell cycle analysis.

Cell cycle progression experiments were then designed to examine the cytostatic effects of new dual inhibitors on LNCaP and PC 3 cells. First, LNCaPs were treated with increasing concentrations of **10a**−**j** and the DNA content was analyzed by cytometry after staining with propidium iodide (Table 3). In control cells, the G1, S, and G2-M populations represented 69, 12, and 15% of the cells, respectively. After incubation with most of the new molecules, a G1-block was observed. Furthermore, **10h** (10 μM) produced the sub-G1 fraction indicative of programmed cell death, while higher concentrations of celecoxib and **10a** were required to observe such an effect (Figure 4A). It is to be noted that rofecoxib did not induce G1-block even at 100 μM treatment. This is to be compared with the lack of antiproliferative activity of this coxib even after 9-day incubation (data not shown). Other authors reported the same results on transformed cells[31] and some[21] demonstrated that the antiproliferative activity profiles exhibited by the novel tricyclic COX-2 inhibitors is dependent on the electronic nature of the central ring system. Taken together, our data led us to assume a promising pharmacological in vitro profile for **10h**. The G1-block caused by celecoxib and all the original structures may be assigned to a decreased expression of cyclins or an increased expression of cell cycle inhibitory proteins as

A

	cell population in cycle phases (%)			
compound	Sub-G1	G1	S	G2-M
untreated control	4.2	69	11.6	15.2
celecoxib[a]	4	**78**	6.9	11.1
10a[b]	3.9	**74.2**	9.9	12
10h[c]	10.8	**74.2**	6.9	8.2

[a] 5.10^{-5} M. [b] 10^{-4} M. [c] 10^{-5} M.

B

	cell population in cycle phases (%)			
compound	Sub-G1	G1	S	G2-M
untreated control	2.9	72.8	6.6	17.6
celecoxib[a]	2.4	68.5	5.8	**23.5**
10a[b]	1.2	67.8	5.1	**25.9**
10h[c]	2.1	71.5	6.6	**19.5**

[a] 5.10^{-5} M. [b] 10^{-4} M. [c] 10^{-5} M.

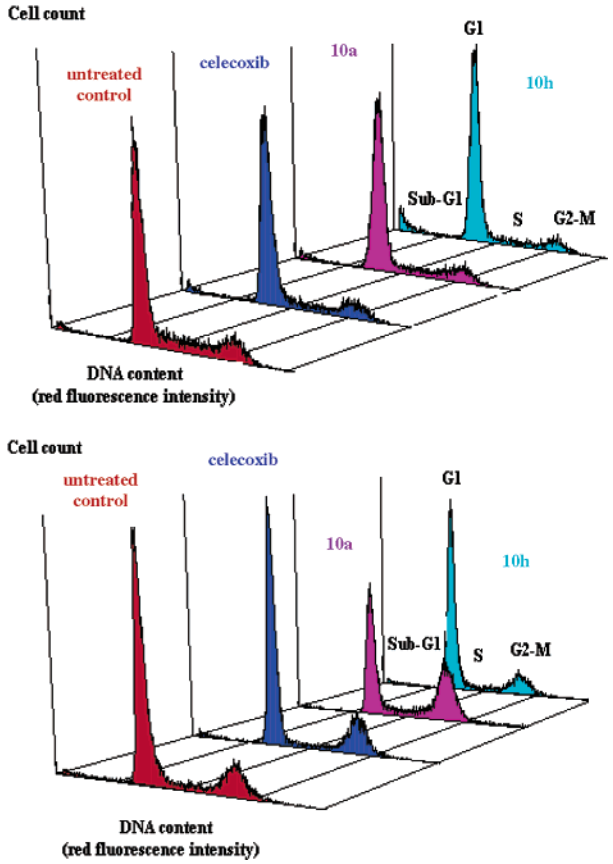

Figure 4. FACS diagram showing the effects of **10a**, **10h**, and celecoxib on LNCaP (A) and PC 3 (B) cells.

in colon cancer cells.[32] However, ceramide changes could also be suspected, as in metastatic breast cancer,[33] since these compounds did not induce a G1-block in PC 3 cells which are known to overexpress ceramidase.[34,35] In these PC 3 cells, **10h** (1 μM) and celecoxib (50 μM) only induced an accumulation of cells in the G2-M phase (Figure 4B), which could be connected to their capacity to decrease EGFR expression (data not shown). Proapoptotic activity was again associated with cellular treatment making use of these two inhibitors. Further experiments will enable us to extend our understanding of mechanisms, but **10h** is already expected to be a convenient tool in the design of new efficient and selective inhibitors. A further modeling study would enlighten structural features and the influence of key chemical groups in relation to antiproliferative and proapoptotic effects.

Conclusions

In contrast to the tremendous amount of work focusing on the therapeutic responses of COX-2 and LOX inhibitors to inflammation diseases, relatively limited information is available concerning their potential use as antitumor agents in the treatment of cancer. Nevertheless, the advantage of COX/LOX inhibition is well-known, especially in human prostate cancer, even if the overexpression and the real participation of COX-2 in this pathology is a subject of controversy.[6,36]

For this purpose, 19 diarylpyrazoles were synthesized, first taking into account the pharmacophoric elements necessary to recognize the main subsites of the active pockets of both enzyme systems. Our data could suggest that the presence of an aminosulfonyl group (as in **10h**) conferred optimal potency against the human prostatic cancer cell lines LNCaP and PC 3. This result can be correlated to those of authors[19,31] that showed that celecoxib, but not rofecoxib, inhibits the growth of transformed cells in vitro. However, the aminosulfonyl-containing counterpart of rofecoxib does not show apoptosis-inducing activity in PC 3 cells.[19] Moreover, only weak structural modifications at the 5-phenyl substituent of celecoxib reduce its apoptosis-inducing activity. Thus, it is not possible to link antitumor activity to only this aminosulfonyl group. The nature of the central ring system of tricyclic inhibitors might be particularly investigated in the same way as structure−function relations on other aromatic rings.

The better activity of **10h** vs **10a** seems to confirm that the structural requirements for the induction of apoptosis are distinct from structural requirements for the mediation of COX-2 inhibition. Mechanisms of antitumor activity remain to be elucidated, but compound **10h** could be considered as a lead compound in the design of a new class of potent drugs. These new molecules could be used as single therapeutics or in cooperation with other cytostatic agents to target effective downstream signaling pathways.

Experimental Section

Chemistry. The abbreviations used are as follows: DMA, *N*,*N*-dimethylacetamide; NBS, *N*-bromosuccinimide. Unless otherwise noted, moisture-sensitive reactions were conducted in dry nitrogen or argon. Tetrahydrofuran was distilled from sodium/benzophenone prior to use. Analytical thin-layer chromatography (TLC) was performed on precoated Kieselgel 60F_{254} plates (Merck); compounds were visualized by UV and/or with iodine. Flash chromatography (FC) was performed with

silica gel Kieselgel Si 60, 0.040−0.063 mm (Merck). Analytical HPLC was carried out on a Kontron 325 System chromatograph equipped with a 440L photodiode array detector using a Kromasil C_{18} 5 μm 150 mm × 4.6 mm column (reverse phase) to determine the purity of the products. Elution was performed with the following two systems: solution A (90% water, 10% acetonitrile) and solution B (10% water, 90% acetonitrile). Melting points were determined with a Büchi 535 capillary melting point apparatus and remain uncorrected. The structures of all compounds were supported by IR (KBr pellets, FT-Bruker Vector 22 instrument) and ^{1}H NMR at 300 MHz on a Bruker DPX-300 spectrometer. Chemical shifts (δ) are reported in ppm downfield from tetramethylsilane, J values are in hertz, and the splitting patterns are designed as follows: s, singlet; d, doublet; t, triplet; q, quartet; m, multiplet; b, broad. APCI$^+$ (atmospheric pressure chemical ionization) mass spectra were obtained on an LC−MS system Thermo Electron Surveyor MSQ. Elemental analyses were performed by the "Service Central d'Analyses" at the CNRS, Vernaison, France.

4-Methanesulfonylphenylhydrazine Hydrochloride[37] **(1a).** A solution of 4-chlorophenylmethyl sulfone (25.5 g, 134 mmol) and hydrazine monohydrate (99 mL, 2 mol) was carefully heated in a Parr shaker at 160 °C for 1 h. After cooling to room temperature, the mixture was diluted with EtOH (100 mL) and the solvent was evaporated under reduced pressure. Ice water (70 mL) was then added and the formed precipitate was washed with water (2 × 10 mL) and collected by filtration. The solid (19.3 g, 104 mmol) was stirred with 37% HCl (8.7 mL, 104 mmol) in ethanol (140 mL) for 0.5 h. The precipitate was collected, washed with EtOH, and air-dried to give **1a** (21.2 g, 73% yield) of sufficient purity to be used without further purification: IR 3156, 3002, 2921, 2678, 1600, 1533 cm^{-1}; ^{1}H NMR (DMSO-d_6) δ 10.7 (bs, 3H), 9.2 (bs, 1H), 7.79 (d, J = 8.9, 2H), 7.11 (d, J = 8.9, 2H), 3.14 (s, 3H).

Ethyl 2-Hydroxy-4-oxo-4-phenyl-2-butenoate[38] **(2).** Ethanol (350 mL) was converted to sodium ethoxide by portionwise addition of sodium (11.8 g, 514 mmol) before a solution of diethyl oxalate (70 mL, 514 mmol) and acetophenone (30 mL, 257 mmol) in ethanol (150 mL) was added dropwise at 50 °C. The mixture was heated at reflux for 2 h. After cooling, the solvent was removed and the residue was taken up in water (1.5 L) and acidified with concentrated HCl (30 mL). The aqueous mixture was extracted with diethyl ether (3 × 1 L). The combined extracts were washed with brine (200 mL), dried ($MgSO_4$), and concentrated. The crude brown oil (57 g) was purified by FC (heptane/AcOEt 7:3) to give **2** (41 g, 72% yield): IR 3063, 2984, 2939, 1747, 1731, 1684, 1599, 1452 cm^{-1}; ^{1}H NMR ($CDCl_3$) δ 15.30 (bs, 1H), 7.96 (d, J = 7.8, 2H), 7.58 (dt, J = 7.2, J = 1.2, 1H), 7.47 (dd, J = 7.8, J = 1.2, 2H), 7.06 (s, 1H), 4.35 (q, J = 7.2, 2H), 1.38 (t, J = 7.2, 3H).

3-Fluoro-5-(4-methoxytetrahydropyran-4-yl)phenol (6). A solution of benzyl alcohol (19 g, 175 mmol) in 220 mL of DMA was stirred while sodium hydride (7.1 g, 60% dispersion in mineral oil, 177 mmol) was added portionwise at 4 °C. The mixture was stirred for 0.5 h and 1-bromo-3,5-difluorobenzene (29.6 g, 154 mmol) was added dropwise. The reaction mixture was stirred, allowed to warm to room temperature overnight, and then poured into water. The aqueous mixture was acidified with 1 N HCl and extracted with diethyl ether (2 L). The organic layer was washed successively with H_2O and brine, dried over $MgSO_4$, and evaporated under vacuum. The residue was purified by FC (heptane) to yield 1-benzyloxy-3-bromo-5-fluorobenzene **3** (27.4 g, 63% yield): IR 3090, 3033, 2922, 2870, 1604, 1585, 1497 cm^{-1}; ^{1}H NMR ($CDCl_3$) δ 7.45−7.38 (m, 5H), 6.98 (m, 1H), 6.89 (d, J = 8.2, 1H), 6.67 (d, J = 8.2, 1H), 5.04 (s, 2H). Butyllithium (43 mL, 2.5 M in hexanes, 107 mmol) was added dropwise at −78 °C in a nitrogen atmosphere to a solution of oily fluorobenzene **3** (27.3 g, 97 mmol) in 500 mL of dry THF. The mixture was stirred for 0.5 h and then 3,4,5,6-tetrahydro-4*H*-pyran-4-one (9.7 g, 97 mmol) dissolved in THF (10 mL) was added dropwise to the solution, which was stirred at −78 °C for 4 h, allowed to warm to 4 °C overnight, and quenched with a saturated NH_4Cl solution (200 mL). The aqueous mixture was extracted with diethyl ether (1 × 500 mL). The organic layer was washed successively with H_2O and brine, dried over $MgSO_4$, and evaporated under vacuum. The residue was purified by FC (heptane/AcOEt 7:3) to give 4-(3-benzyloxy-5-fluorophenyl)tetrahydropyran-4-ol **4** (19.3 g, 66% yield): IR 3404, 3033, 2955, 2870, 1620, 1590, 1140 cm^{-1}; ^{1}H NMR ($CDCl_3$) δ 7.41−7.34 (m, 5H), 6.93 (m, 1H), 6.82 (d, J = 8.1, 1H), 6.61 (d, J = 8.1, 1H), 5.05 (s, 2H), 3.94−3.81 (m, 4H), 2.10 (m, 2H), 1.81 (bs, 1H), 1.62 (m, 2H). Sodium hydride (2.6 g, 60% dispersion in mineral oil, 66.1 mmol) was added portionwise at 4 °C to a solution of oily alcohol **4** (19 g, 63.8 mmol) and iodomethane (10.8 g, 75.4 mmol) in 30 mL of DMF. The mixture was stirred for 3 h at room temperature. The reaction was quenched by adding water, and the aqueous phase was extracted with diethyl ether (1 L). The organic layer was washed with brine, dried over $MgSO_4$, and evaporated under vacuum. Purification was performed by FC (heptane/AcOEt 8:2) to yield 13.4 g (67% yield) of 4-(3-benzyloxy-5-fluorophenyl)-4-methoxytetrahydropyran **5**: IR 3065, 3033, 2953, 2866, 2825, 1615, 1590 cm^{-1}; ^{1}H NMR ($CDCl_3$) δ 7.47−7.34 (m, 5H), 6.84 (m, 1H), 6.74 (d, 1H), 6.44 (d, J = 8.1, 1H), 5.07 (s, 2H), 3.90−3.83 (m, 4H), 3.25 (s, 3H), 2.04−1.83 (m, 4H). A solution of oily ether **5** (13 g, 41 mmol) and palladium hydroxide (20% on carbon, 1 g) in 170 mL of ethanol was stirred under atmospheric hydrogen pressure for 15 h at room temperature. The reaction mixture was filtered off on Celite 245 to remove the insoluble materials. The filtrate was then concentrated in a vacuum to give **6** as an oil (8.7 g, 94% yield) that was used without further purification: IR 3242, 2967, 2942, 2880, 1610 cm^{-1}; ^{1}H NMR ($CDCl_3$) δ 6.90 (m, 1H), 6.69−6.65 (m, 2H), 6.51 (d, J = 9.6, 1H), 3.90−3.88 (m, 4H), 3.03 (s, 3H), 2.07−1.92 (m, 4H).

3-Ethoxycarbonyl-1-(4-methanesulfonylphenyl)-5-phenyl-1*H*-pyrazole (7a) was generated in 80% yield (39.6 g) from ester **2** (31.0 g, 1.34 mol) and arylhydrazine hydrochloride **1a** (29.8 g, 1.34 mol) in 1.3 L of absolute ethanol at reflux for 3 h and cooling to 20 °C: mp 170 °C (ethanol); IR 3129, 2996, 2916, 1716, 1596, 1232 cm^{-1}; ^{1}H NMR (DMSO-d_6) δ 8.00 (d, J = 8.7, 2H), 7.60 (d, J = 9.0, 2H), 7.44−7.40 (m, 3H), 7.35−7.30 (m, 2H), 7.18 (s, 1H), 4.35 (q, J = 7.0, 2H), 3.29 (s, 3H), 1.33 (t, J = 7.0, 3H).

General Procedure for the Synthesis of Pyrazoles 7b−j (Procedure A). A solution of ester **2** (2.5 mL, 2 M in EtOH, 5 mmol) was added to a solution of arylhydrazines **1b−j** (5.25 mmol) in EtOH (10 mL) in a multiblock reactor. The reaction mixture was refluxed for 3 h and the solvent was removed. After cooling to 20 °C, the residue was taken up into brine (3 mL) and the aqueous mixture was extracted with ethyl acetate (2 × 10 mL). The combined extracts were concentrated, and the crude product was purified by FC (cyclohexane/AcOEt in adequate proportions) to give the 1,5-diarylpyrazoles **7b−j**.

3-Ethoxycarbonyl-1,5-diphenyl-1*H*-pyrazole (7b) was synthesized as an oil (1.14 g, 76% yield) from ester **2** (2.5 mL, 2 M in EtOH, 5 mmol) and phenylhydrazine (0.77 g, 5.25 mmol) by procedure A and purification by FC with cyclohexane/AcOEt 9:1: IR 3129, 2978, 1714, 1596, 1501, 1234 cm^{-1}; ^{1}H NMR ($CDCl_3$) δ 7.45−7.20 (m, 10H), 7.06 (s, 1H), 4.46 (q, J = 7.1, 2H), 1.44 (t, J = 7.1, 3H).

3-Ethoxycarbonyl-1-(4-fluorophenyl)-5-phenyl-1*H*-pyrazole (7c) was synthesized as an oil (1.4 g, 93% yield) from ester **2** (2.5 mL, 2 M in EtOH, 5 mmol) and 4-fluorophenylhydrazine (0.87 g, 5.25 mmol) by procedure A and purification by FC with cyclohexane/AcOEt 9:1: IR 3084, 2985, 1736, 1606, 1512, 1223 cm^{-1}; ^{1}H NMR ($CDCl_3$) δ 7.45−7.27 (m, 5H), 7.22−7.19 (m, 2H), 7.07−7.02 (m, 3H), 4.46 (q, J = 7.1, 2H), 1.43 (t, J = 7.1, 3H).

1-(4-Chlorophenyl)-3-ethoxycarbonyl-5-phenyl-1*H*-pyrazole (7d) was synthesized as an oil (1.5 g, 94% yield) from ester **2** (2.5 mL, 2 M in EtOH, 5 mmol) and 4-chlorophenylhydrazine (0.9 g, 5.25 mmol) by procedure A and purification by FC with cyclohexane/AcOEt 9:1: IR 3142, 2986, 1716, 1498, 1230 cm^{-1}; ^{1}H NMR ($CDCl_3$) δ 7.36−7.29 (m, 7H), 7.27−7.20 (m, 2H), 7.04 (s, 1H), 4.47 (q, J = 7.1, 2H), 1.43 (t, J = 7.1, 3H).

3-Ethoxycarbonyl-1-(4-methylphenyl)-5-phenyl-1*H*-pyrazole (7e) was synthesized as an oil (1.2 g, 80% yield) from ester **2** (2.5 mL, 2 M in EtOH, 5 mmol) and 4-methylphenylhydrazine (0.85 g, 5.25 mmol) by procedure A and purification by FC with cyclohexane/AcOEt 9:1: IR 3128, 2979, 1712, 1517, 1231 cm^{-1}; ^1H NMR ($CDCl_3$) δ 7.33−7.27 (m, 3H), 7.24−7.20 (m, 4H), 7.14 (d, J = 8.0, 2H), 7.04 (s, 1H), 4.46 (q, J = 7.1, 2H), 2.36 (s, 3H), 1.43 (t, J = 7.1, 3H).

3-Ethoxycarbonyl-1-(4-methoxyphenyl)-5-phenyl-1*H*-pyrazole (7f) was synthesized as an oil (1.25 g, 78% yield) from ester **2** (2.5 mL, 2 M in EtOH, 5 mmol) and 4-methoxyphenylhydrazine (0.93 g, 5.25 mmol) by procedure A and purification by FC with cyclohexane/AcOEt 4:1: IR 2961, 2837, 1708, 1607, 1516, 1230 cm^{-1}; ^1H NMR ($CDCl_3$) δ 7.33−7.20 (m, 7H), 7.04 (s, 1H), 6.86 (dd, J = 9.2, J = 2.4, 2H), 4.46 (q, J = 7.2, 2H), 3.82 (s, 3H), 1.43 (t, J = 7.2, 3H).

3-Ethoxycarbonyl-1-(4-trifluoromethoxyphenyl)-5-phenyl-1*H*-pyrazole (7g) was synthesized as an oil (1.5 g, 79% yield) from ester **2** (2.5 mL, 2 M in EtOH, 5 mmol) and 4-trifluoromethoxyphenylhydrazine (1.22 g, 5.25 mmol) by procedure A and purification by FC with cyclohexane/AcOEt 9:1: IR 3136, 2991, 1717, 1513, 1270, 1233 cm^{-1}; ^1H NMR ($CDCl_3$) δ 7.41−7.32 (m, 5H), 7.24−7.19 (m, 4H), 7.05 (s, 1H), 4.47 (q, J = 7.0, 2H), 1.44 (t, J = 7.0, 3H).

1-(4-Aminosulfonylphenyl)-3-ethoxycarbonyl-5-phenyl-1*H*-pyrazole (7h) was synthesized as an oil (1.17 g, 62% yield) from ester **2** (2.5 mL, 2 M in EtOH, 5 mmol) and 4-aminosulfonylphenylhydrazine (1.21 g, 5.25 mmol) by procedure A and purification by FC with heptane/AcOEt 6:4: IR 3321, 3242, 3124, 2990, 2925, 1723, 1595, 1347, 1230, 1173 cm^{-1}; ^1H NMR ($CDCl_3$) δ 7.87 (dd, J = 8.8, J = 2.0, 2H), 7.45 (dd, J = 8.8, J = 2.0, 2H), 7.40−7.33 (m, 3H), 7.24−7.20 (m, 2H), 7.04 (s, 1H), 5.26 (s, 2H), 4.45 (q, J = 7.1, 2H), 1.43 (t, J = 7.1, 3H).

3-Ethoxycarbonyl-1-(3,4-dimethylphenyl)-5-phenyl-1*H*-pyrazole (7i) was synthesized as an oil (1.2 g, 75% yield) from ester **2** (2.5 mL, 2 M in EtOH, 5 mmol) and 3,4-dimethylphenylhydrazine (0.93 g, 5.25 mmol) by procedure A and purification by FC with cyclohexane/AcOEt 85:15: IR 3128, 2985, 1711, 1610, 1236, 769 cm^{-1}; ^1H NMR ($CDCl_3$) δ 7.33−7.21 (m, 6H), 7.05−7.03 (m, 2H), 6.91 (dd, J = 8.1, J = 2.0, 1H), 4.46 (q, J = 7.2, 2H), 2.26 (s, 3H), 2.23 (s, 3H), 1.43 (t, J = 7.2, 3H).

1-(3,4-Dichlorophenyl)-3-ethoxycarbonyl-5-phenyl-1*H*-pyrazole (7j) was synthesized as an oil (1.5 g, 83% yield) from ester **2** (2.5 mL, 2 M in EtOH, 5 mmol) and 3,4-dichlorophenylhydrazine (1.15 g, 5.25 mmol) by procedure A and purification by FC with cyclohexane/AcOEt 9:1: IR 3134, 2987, 1720, 1591, 1477, 1227 cm^{-1}; ^1H NMR ($CDCl_3$) δ 7.61 (d, J = 2.3, 1H), 7.41−7.34 (m, 4H), 7.26−7.22 (m, 2H), 7.07 (dd, J = 8.7, J = 2.3, 1H), 7.04 (s, 1H), 4.47 (q, J = 7.0, 2H), 1.44 (t, J = 7.0, 3H).

3-Hydroxymethyl-1-(4-methanesulfonylphenyl)-5-phenyl-1*H*-pyrazole (8a). $LiBH_4$ (54 mL, 2 M in THF, 0.11 mol) was added dropwise under argon, with rapid stirring, to a solution of ester **7a** (20.0 g, 54 mmol) in 300 mL of THF. The mixture was stirred vigorously for 72 h at room temperature. Acetone (8 mL) and water (2 mL) were added successively at 4 °C and the solvents were removed. The residue was taken up into ethyl acetate (600 mL) and washed with water (100 mL) and brine (50 mL). The organic layer was dried ($MgSO_4$) and concentrated to give **8a** (17.0 g, 95% yield), which was used without further purification: mp 133−134 °C; IR 3355, 2997, 2919, 1594, 1505, 1152 cm^{-1}; ^1H NMR ($CDCl_3$) δ 7.88 (d, J = 8.5, 2H), 7.49 (d, J = 8.8, 2H), 7.42−7.34 (m, 3H), 7.33−7.21 (m, 2H), 6.56 (s, 1H), 4.80 (s, 2H), 3.06 (s, 3H).

3-Bromomethyl-1-(4-methanesulfonylphenyl)-5-phenyl-1*H*-pyrazole (9a). Triphenylphosphine (12.5 g, 47.5 mmol) was added at 0 °C to a stirred solution of alcohol **8a** (12.0 g, 36.5 mmol) in 300 mL of dry CH_2Cl_2. After 0.5 h, NBS (7.2 g, 40.2 mmol) was added portionwise and the mixture was stirred for 15 h at room temperature. The solvent was evaporated under reduced pressure to provide a crude product which was purified by FC (cyclohexane/AcOEt 1:1) to give alkyl bromide **9a** (12.2 g, 85% yield): mp 158−159 °C; IR 3003, 2923, 1590, 1546, 1503 cm^{-1}; ^1H NMR ($CDCl_3$) δ 7.90 (d, J = 8.6, 2H), 7.50 (d, J = 8.6, 2H), 7.42−7.34 (m, 3H), 7.27−7.23 (m, 2H), 6.62 (s, 1H), 4.57 (s, 2H), 3.06 (s, 3H).

General Procedure for the Synthesis of Bromomethylpyrazoles 9b−j (Procedure B). $LiBH_4$ (5 mL, 2 M in THF, 10 mmol) was added dropwise under argon to a solution of 1,5-diarylpyrazoles **7b−j** (3−5 mmol) in 15 mL of THF in a multiblock reactor. The mixture was stirred vigorously for 72 h at room temperature. Acetone (1 mL) and brine (0.2 mL) were added successively, and the reaction mixture was stirred at 20 °C for 1 h before the solvent was removed. The residue was dried under vacuum (P_2O_5) for 15 h. The crude anhydrous primary alcohols **8b−j** were taken up into CH_2Cl_2 (15 mL) before addition of $MgSO_4$ (0.5 g, 4.1 mmol). Triphenylphosphine (1.7 g, 6.5 mmol) was added at 0 °C before NBS (1 g, 5.5 mmol) was added portionwise after 0.5 h and the mixture stirred for 15 h at room temperature. The solvent was evaporated under reduced pressure to give a crude product which was purified by FC (cyclohexane/AcOEt in adequate proportions) to give the 1,5-diarylpyrazoles **9b−j**.

3-Bromomethyl-1,5-diphenyl-1*H*-pyrazole (9b) was synthesized as an oil (340 mg, 28% yield) from ester **7b** (1.1 g, 3.76 mmol) by procedure B and purification by FC with cyclohexane/AcOEt 7:3: IR 3058, 2924, 1594, 1503 cm^{-1}; ^1H NMR ($CDCl_3$) δ 7.37−7.22 (m, 10H), 6.60 (s, 1H), 4.61 (s, 2H).

3-Bromomethyl-1-(4-fluorophenyl)-5-phenyl-1*H*-pyrazole (9c) was synthesized as an oil (360 mg, 24% yield) from ester **7c** (1.35 g, 4.35 mmol) by procedure B and purification by FC with cyclohexane/AcOEt 7:3: IR 3072, 2925, 1514 cm^{-1}; ^1H NMR ($CDCl_3$) δ 7.34−7.20 (m, 7H), 7.07−7.00 (m, 2H), 6.60 (s, 1H), 4.59 (s, 2H).

3-Bromomethyl-1-(4-chlorophenyl)-5-phenyl-1*H*-pyrazole (9d) was synthesized as an oil (380 mg, 22% yield) from ester **7d** (1.45 g, 4.44 mmol) by procedure B and purification by FC with cyclohexane/AcOEt 7:3: IR 3070, 2925, 1500 cm^{-1}; ^1H NMR ($CDCl_3$) δ 7.36−7.21 (m, 9H), 6.59 (s, 1H), 4.58 (s, 2H).

3-Bromomethyl-1-(4-methylphenyl)-5-phenyl-1*H*-pyrazole (9e) was synthesized as an oil (360 mg, 28% yield) from ester **7e** (1.15 g, 3.75 mmol) by procedure B and purification by FC with cyclohexane/AcOEt 7:3: IR 3038, 2923, 1515 cm^{-1}; ^1H NMR ($CDCl_3$) δ 7.34−7.12 (m, 9H), 6.58 (s, 1H), 4.60 (s, 2H), 2.36 (s, 3H).

3-Bromomethyl-1-(4-methoxyphenyl)-5-phenyl-1*H*-pyrazole (9f) was synthesized as an oil (380 mg, 30% yield) from ester **7f** (1.20 g, 3.72 mmol) by procedure B and purification by FC with cyclohexane/AcOEt 7:3: IR 3058, 2932, 2836, 1609, 1589, 1547, 1515 cm^{-1}; ^1H NMR ($CDCl_3$) δ 7.32−7.20 (m, 7H), 6.87−6.84 (m, 2H), 6.58 (s, 1H), 4.60 (s, 2H), 3.82 (s, 3H).

3-Bromomethyl-1-(4-trifluoromethoxyphenyl)-5-phenyl-1*H*-pyrazole (9g) was synthesized as an oil (440 mg, 28% yield) from ester **7g** (1.45 g, 3.85 mmol) by procedure B and purification by FC with cyclohexane/AcOEt 9:1: IR 3063, 2926, 2855, 1606, 1577, 1550, 1513 cm^{-1}; ^1H NMR ($CDCl_3$) δ 7.36−7.31 (m, 5H), 7.27−7.18 (m, 4H), 6.60 (s, 1H), 4.58 (s, 2H).

1-(4-Aminosulfonylphenyl)-3-bromomethyl-5-phenyl-1*H*-pyrazole (9h) was synthesized as an oil (400 mg, 33% yield) from ester **7h** (1.12 g, 3.0 mmol) by procedure B and purification by FC with cyclohexane/AcOEt 6:4: IR 3297, 3094, 2924, 1593, 1545, 1502 cm^{-1}; ^1H NMR (DMSO-d_6) δ 7.84−7.81 (m, 2H), 7.73−7.16 (m, 9H), 6.79 (s, 1H), 4.82 (s, 2H).

3-Bromomethyl-1-(3,4-dimethylphenyl)-5-phenyl-1*H*-pyrazole (9i) was synthesized as an oil (600 mg, 48% yield) from ester **7i** (1.15 g, 3.6 mmol) by procedure B and purification by FC with cyclohexane/AcOEt 9:1: IR 3056, 2961, 2923, 2854, 1611, 1584, 1547, 1506 cm^{-1}; ^1H NMR ($CDCl_3$) δ 7.33−7.22 (m, 5H), 7.20 (d, J = 2.3, 1H), 7.04 (d, J = 7.9, 1H), 6.87 (dd, J = 8.2, J = 2.3, 1H), 6.58 (s, 1H), 4.60 (s, 2H), 2.26 (s, 3H), 2.24 (s, 3H).

3-Bromomethyl-1-(3,4-dichlorophenyl)-5-phenyl-1*H*-pyrazole (9j) was synthesized as an oil (550 mg, 36% yield) from ester **7j** (1.45 g, 4.0 mmol) by procedure B and purification by FC with cyclohexane/AcOEt 7:3: IR 3093, 2924, 2852, 1593,

1545, 1478 cm^{-1}; ^1H NMR ($CDCl_3$) δ 7.54 (d, J = 2.5, 1H), 7.43−7.23 (m, 6H), 7.03 (dd, J = 8.6, J = 2.5, 1H), 6.60 (s, 1H), 4.69 (s, 2H).

3-[3-Fluoro-5-(4-methoxytetrahydropyran-4-yl)phenoxymethyl]-1-(4-methanesulfonylphenyl)-5-phenyl-1*H*-pyrazole (10a). A solution of phenol **6** (4.45 g, 19.7 mmol) in 35 mL of DMF was stirred while cesium carbonate (6.7 g, 20.6 mmol) was added rapidly at room temperature. The mixture was stirred for 0.5 h and then alkyl bromide **9a** (7.0 g, 19.9 mmol) was added in one batch. The reaction mixture was stirred at 90 °C for 2 h, concentrated under reduced pressure, and extracted with ethyl acetate. The organic phase was washed with brine, dried ($MgSO_4$), and concentrated under vacuum. Purification was performed by FC (cyclohexane/AcOEt 1:1) to yield, after vacuum-drying, pyrazole **10a** (8.5 g, 88% yield): mp 70−72 °C; IR 3062, 2951, 2865, 1614, 1593 cm^{-1}; ^1H NMR ($CDCl_3$) δ 7.91 (d, J = 8.9, 2H), 7.52 (d, J = 8.6, 2H), 7.41−7.34 (m, 3H), 7.27−7.24 (m, 2H), 6.90 (s, 1H), 6.77−6.70 (m, 2H), 6.67 (s, 1H), 5.18 (s, 2H), 3.85−3.81 (m, 4H), 3.10 (s, 3H), 3.07 (s, 3H), 2.00 (m, 4H); LC−MS ($APCI^+$) m/z 537 (MH^+). Anal. ($C_{29}H_{29}FN_2O_5S$) C, H, N.

General Procedure for the Synthesis of Ethers 10b−j (Procedure C). The 1-arylpyrazoles **9b−j** (0.5 mmol) were added in a multiblock reactor to a suspension of phenol **6** (1.1 mL, 0.5 M in DMF, 0.55 mmol) and cesium carbonate (0.21 g, 0.58 mmol) in DMF (0.5 mL). The reaction mixture was stirred at 90 °C for 1 h before the solvent was removed. After cooling to 20 °C, the residue was taken up in brine (3 mL) and the aqueous mixture was extracted with ethyl acetate (2 × 10 mL). The combined extracts were concentrated, and the crude product was purified by FC (cyclohexane/AcOEt in adequate proportions) to yield the phenoxymethylpyrazoles **10b−j**.

3-[3-Fluoro-5-(4-methoxytetrahydropyran-4-yl)phenoxymethyl]-1,5-diphenyl-1*H*-pyrazole (10b) was synthesized as an oil (210 mg, 91% yield) from alkyl bromide **9b** (157 mg, 0.5 mmol) and phenol **6** by procedure C and purification by FC with cyclohexane/AcOEt 8:2: IR 3060, 2923, 2853, 1616, 1592, 1506 cm^{-1}; ^1H NMR ($CDCl_3$) δ 7.36−7.22 (m, 10H), 6.92 (m, 1H), 6.76 (m, 1H), 6.72 (m, 1H), 6.64 (s, 1H), 5.19 (s, 2H), 3.86−3.82 (m, 4H), 2.99 (s, 3H), 2.04−1.90 (m, 4H); LC−MS ($APCI^+$) m/z 459 (MH^+). Anal. ($C_{28}H_{27}FN_2O_3$) C, H, N.

3-[3-Fluoro-5-(4-methoxytetrahydropyran-4-yl)phenoxymethyl]-1-(4-fluorophenyl)-5-phenyl-1*H*-pyrazole (10c) was synthesized in 55% yield (130 mg) from alkyl bromide **9c** (166 mg, 0.5 mmol) and phenol **6** by procedure C and purification by FC with cyclohexane/AcOEt 8:2: mp 81−83 °C; IR 3081, 2922, 2859, 1612, 1598, 1513 cm^{-1}; ^1H NMR ($CDCl_3$) δ 7.34−7.21 (m, 7H), 7.08−7.02 (m, 2H), 6.91 (m, 1H), 6.76−6.71 (m, 2H), 6.63 (s, 1H), 5.17 (s, 2H), 3.86−3.82 (m, 4H), 3.00 (s, 3H), 2.04−1.95 (m, 4H); LC−MS ($APCI^+$) m/z 477 (MH^+). Anal. ($C_{28}H_{26}F_2N_2O_3$) C, H, N.

1-(4-Chlorophenyl)-3-[3-fluoro-5-(4-methoxytetrahydropyran-4-yl)phenoxymethyl]-5-phenyl-1*H*-pyrazole (10d) was synthesized in 50% yield (120 mg) from alkyl bromide **9d** (174 mg, 0.5 mmol) and phenol **6** by procedure C and purification by FC with cyclohexane/AcOEt 8:2: mp 103−105 °C; IR 3063, 2952, 2859, 1613, 1598, 1503 cm^{-1}; ^1H NMR ($CDCl_3$) δ 7.35−7.31 (m, 5H), 7.27−7.22 (m, 4H), 6.91 (m, 1H), 6.75−6.71 (m, 2H), 6.63 (s, 1H), 5.17 (s, 2H), 3.85−3.82 (m, 4H), 3.00 (s, 3H), 2.04−1.90 (m, 4H); LC−MS ($APCI^+$) m/z 494 (MH^+). Anal. ($C_{28}H_{26}ClFN_2O_3$) C, H, N.

3-[3-Fluoro-5-(4-methoxytetrahydropyran-4-yl)phenoxymethyl]-1-(4-methylphenyl)-5-phenyl-1*H*-pyrazole (10e) was synthesized in 85% yield (200 mg) from alkyl bromide **9e** (164 mg, 0.5 mmol) and phenol **6** by procedure C and purification by FC with cyclohexane/AcOEt 8:2: mp 90−92 °C; IR 2951, 2923, 2858, 1612, 1598, 1518 cm^{-1}; ^1H NMR ($CDCl_3$) δ 7.33−7.13 (m, 9H), 6.91 (m, 1H), 6.75 (m, 1H), 6.71 (m, 1H), 6.62 (s, 1H), 5.17 (s, 2H), 3.88−3.79 (m, 4H), 2.99 (s, 3H), 2.37 (s, 3H), 2.04−1.90 (m, 4H); LC−MS ($APCI^+$) m/z 473 (MH^+). Anal. ($C_{29}H_{29}FN_2O_3$) C, H, N.

3-[3-Fluoro-5-(4-methoxytetrahydropyran-4-yl)phenoxymethyl]-1-(4-methoxyphenyl)-5-phenyl-1*H*-pyrazole (10f) was synthesized in 82% yield (200 mg) from alkyl bromide **9f** (172 mg, 0.5 mmol) and phenol **6** by procedure C and purification by FC with cyclohexane/AcOEt 8:2: mp 108−110 °C; IR 3054, 2956, 2929, 2866, 1612, 1597, 1517 cm^{-1}; ^1H NMR ($CDCl_3$) δ 7.32−7.21 (m, 7H), 6.91 (m, 1H), 6.89−6.84 (m, 2H), 6.75 (m, 1H), 6.72 (m, 1H), 6.62 (s, 1H), 5.17 (s, 2H), 3.82 (s, 3H), 2.99 (s, 3H), 2.04−1.90 (m, 4H); LC−MS ($APCI^+$) m/z 489 (MH^+). Anal. ($C_{29}H_{29}FN_2O_4$) C, H, N.

1-(4-Trifluoromethoxyphenyl)-3-[3-fluoro-5-(4-methoxytetrahydropyran-4-yl)phenoxymethyl]-5-phenyl-1*H*-pyrazole (10g) was synthesized in 74% yield (200 mg) from alkyl bromide **9g** (200 mg, 0.5 mmol) and phenol **6** by procedure C and purification by FC with cyclohexane/AcOEt 8:2: mp 71−73 °C; IR 3071, 2950, 2873, 1613, 1600, 1514 cm^{-1}; ^1H NMR ($CDCl_3$) δ 7.37−7.34 (m, 5H), 7.26−7.19 (m, 4H), 6.91 (m, 1H), 6.77−6.70 (m, 2H), 6.64 (s, 1H), 5.17 (s, 2H), 3.88−3.82 (m, 4H), 3.00 (s, 3H), 2.04−1.95 (m, 4H); LC−MS ($APCI^+$) m/z 543 (MH^+). Anal. ($C_{29}H_{26}F_4N_2O_4$) C, H, N.

1-(4-Aminosulfonylphenyl)-3-[3-fluoro-5-(4-methoxytetrahydropyran-4-yl)phenoxymethyl]-5-phenyl-1*H*-pyrazole (10h) was synthesized in 72% yield (190 mg) from alkyl bromide **9h** (196 mg, 0.5 mmol) and phenol **6** by procedure C and purification by FC with cyclohexane/AcOEt 1:1: mp 68−70 °C; IR 3415, 3076, 2923, 2853, 1616, 1593, 1506 cm^{-1}; ^1H NMR ($CDCl_3$) δ 7.90 (d, 2H), 7.50−7.35 (m, 5H), 7.30−7.25 (m, 4H), 6.91 (m, 1H), 6.75−6.70 (m, 2H), 6.65 (s, 1H), 5.18 (s, 2H), 3.84−3.81 (m, 4H), 2.99 (s, 3H), 2.04−1.90 (m, 4H); LC−MS ($APCI^+$) m/z 538 (MH^+). Anal. ($C_{28}H_{28}FN_3O_5S$) C, H, N.

3-[3-Fluoro-5-(4-methoxytetrahydropyran-4-yl)phenoxymethyl]-1-(3,4-dimethylphenyl)-5-phenyl-1*H*-pyrazole (10i) was synthesized as an oil (170 mg, 70% yield) from alkyl bromide **9i** (171 mg, 0.5 mmol) and phenol **6** by procedure C and purification by FC with cyclohexane/AcOEt 4:1: IR 3060, 2925, 2862, 1614, 1590, 1508 cm^{-1}; ^1H NMR ($CDCl_3$) δ 7.35−7.22 (m, 6H), 7.05 (d, J = 8.2, 1H), 6.92−6.87 (m, 2H), 6.75−6.71 (m, 2H), 6.62 (s, 1H), 5.18 (s, 2H), 3.86−3.82 (m, 4H), 2.99 (s, 3H), 2.27 (s, 3H), 2.24 (s, 3H), 2.04−1.91 (m, 4H); LC−MS ($APCI^+$) m/z 487 (MH^+). Anal. ($C_{30}H_{31}FN_2O_3$) C, H, N.

1-(3,4-Dichlorophenyl)-3-[3-fluoro-5-(4-methoxytetrahydropyran-4-yl)phenoxymethyl]-5-phenyl-1*H*-pyrazole (10j) was synthesized in 61% yield (160 mg) from alkyl bromide **9j** (191 mg, 0.5 mmol) and phenol **6** by procedure C and purification by FC with cyclohexane/AcOEt: mp 79−81 °C; IR 3062, 2925, 2859, 1616, 1591, 1478 cm^{-1}; ^1H NMR ($CDCl_3$) δ 7.56 (d, J = 2.5, 1H), 7.40−7.34 (m, 4H), 7.27−7.23 (m, 2H), 7.05 (d, J = 8.8, J = 2.5, 1H), 6.91 (m, 1H), 6.77−6.69 (m, 2H), 6.63 (s, 1H), 5.16 (s, 2H), 3.86−3.82 (m, 4H), 3.00 (s, 3H), 2.00−1.90 (m, 4H); LC−MS ($APCI^+$) m/z 528 (MH^+). Anal. ($C_{28}H_{25}Cl_2FN_2O_3$) C, H, N, Cl.

General Procedure for the Synthesis of Ethers 10k−m (Procedure D). A solution of pyrazole **8a** (1 g, 3.05 mmol) in DMA (3 mL) was stirred while sodium hydride (0.13 g, 60% dispersion in mineral oil, 3.15 mmol) was added rapidly at 0 °C. The mixture was stirred for 0.5 h before a solution of adequate substituted fluorobenzene (3 mmol) in DMA (1 mL) was added in a multiblock reactor. The reaction mixture was stirred at 20 °C for 15 h and the solvent was removed. The residue was taken up in brine (3 mL) and the aqueous mixture was extracted with ethyl acetate (2 × 10 mL). The combined extracts were concentrated, and the crude product was purified by FC (cyclohexane/AcOEt 7:3) to give the phenoxymethylpyrazoles **10k-m**.

3-[(3-Fluoro-5-methoxy)phenoxymethyl]-1-(4-methanesulfonylphenyl)-5-phenyl-1*H*-pyrazole (10k) was synthesized in 20% yield (195 mg) from primary alcohol **8a** and 3,5-difluoroanisole (441 mg, 3 mmol) by procedure D and purification by FC: mp 96−98 °C; IR 3001, 2954, 2925, 2832, 1597, 1511 cm^{-1}; ^1H NMR ($CDCl_3$) δ 7.91 (d, J = 8.2, 2H), 7.52 (d, J = 8.2, 2H), 7.39−7.34 (m, 3H), 7.27−7.23 (m, 2H), 6.65 (s, 1H), 6.43−6.38 (m, 2H), 6.30 (dd, J = 10.2, J = 2.0, 1H), 5.14 (s, 2H), 3.78 (s, 3H), 3.07 (s, 3H); LC−MS ($APCI^+$) m/z 453 (MH^+). Anal. ($C_{24}H_{21}FN_2O_4S$) C, H, N.

1-(4-Methanesulfonylphenyl)-3-[(3-nitro)phenoxymethyl]-5-phenyl-1*H*-pyrazole (10l) was synthesized in 23%

yield (210 mg) from primary alcohol **8a** and 3-fluoronitrobenzene (436 mg, 3 mmol) by procedure D and purification by FC: mp 129−131 °C; IR 3076, 2924, 1595, 1529 cm^{-1}; ^1H NMR ($CDCl_3$) δ 7.87 (m, 4H), 7.52 (m, 3H), 7.41−7.34 (m, 4H), 7.27−7.23 (m, 2H), 6.66 (s, 1H), 5.27 (s, 2H), 3.07 (s, 3H); LC−MS ($APCI^+$) *m/z* 450 (MH^+). Anal. ($C_{23}H_{19}N_3O_5S$) C, H, N.

3-[(5-Cyano-3-fluoro)phenoxymethyl]-1-(4-methanesulfonylphenyl)-5-phenyl-1*H*-pyrazole (10m) was synthesized in 46% yield (410 mg) from primary alcohol **8a** and 3,5-difluorobenzonitrile (422 mg, 3 mmol) by procedure D and purification by FC: mp 62−64 °C; IR 3084, 2924, 2851, 1591, 1506 cm^{-1};^1H NMR δ ($CDCl_3$) 7.92 (d, J = 8.0, 2H), 7.51 (d, J = 8.0, 2H), 7.40 (m, 3H), 7.26 (m, 2H), 7.15 (s, 1H), 7.04 (m, 2H), 6.63 (s, 1H), 5.21 (s, 2H), 3.08 (s, 3H); LC−MS ($APCI^+$) *m/z* 448 (MH^+). Anal. ($C_{24}H_{18}FN_3O_3S$) C, H, N.

General Procedure for the Synthesis of Ethers 10n−s (Procedure E). A solution of pyrazole **9a** (3.3 mL, 0.6 M in DMF, 2 mmol) was added to a solution of adequate substituted phenol (2.2 mmol) and cesium carbonate (0.82 g, 2.3 mmol) in DMF (3 mL) in a multiblock reactor. The reaction mixture was stirred at 90 °C for 1 h and the solvent was removed. After cooling to 20 °C, the residue was taken up in brine (3 mL) and the aqueous mixture was extracted with ethyl acetate (2 × 10 mL). The combined extracts were concentrated and the crude product was purified by FC (cyclohexane/AcOEt 6:4) to give the phenoxymethylpyrazoles **10n−s**.

1-(4-Methanesulfonylphenyl)-3-[3-(4-morpholino)phenoxymethyl]-5-phenyl-1*H*-pyrazole (10n) was synthesized in 74% yield (730 mg) from alkyl bromide **9a** and 3-(4-morpholino)phenol (406 mg, 2.2 mmol) by procedure E and purification by FC: mp 170−172 °C; IR 3060, 2956, 2910, 2852, 1595, 1503 cm^{-1}; ^1H NMR ($CDCl_3$) δ 7.85 (d, J = 8.4, 2H), 7.51 (d, J = 8.4, 2H), 7.40−7.35 (m, 3H), 7.27−7.20 (m, 3H), 6.68 (s, 1H), 6.62−6.57 (m, 3H), 5.18 (s, 2H), 3.86 (t, J = 4.8, 4H), 3.17 (t, J = 4.8, 4H), 3.07 (s, 3H); LC−MS ($APCI^+$) *m/z* 490 (MH^+). Anal. ($C_{27}H_{27}N_3O_4S$) C, H, N.

1-(4-Methanesulfonylphenyl)-3-[(3,4,5-trimethoxy)phenoxymethyl]-5-phenyl-1*H*-pyrazole (10o) was synthesized in 67% yield (660 mg) from alkyl bromide **9a** and 3,4,5-trimethoxyphenol (418 mg, 2.2 mmol) by procedure E and purification by FC: mp 163−165 °C; IR 3061, 2999, 2927, 2838, 1595, 1505 cm^{-1}; ^1H NMR δ ($CDCl_3$) 7.90 (dd, J = 8.8, J = 2.1, 2H), 7.51 (dd, J = 8.8, J = 2.1, 2H), 7.39−7.34 (m, 3H), 7.27−7.24 (m, 2H), 6.68 (s, 1H), 6.33 (s, 2H), 5.16 (s, 2H), 3.86 (s, 6H), 3.81 (s, 3H), 3.07 (s, 3H); LC−MS ($APCI^+$) *m/z* 495 (MH^+). Anal. ($C_{26}H_{26}N_2O_6S$) C, H, N.

3-[(3-Ethoxy)phenoxymethyl]-1-(4-methanesulfonylphenyl)-5-phenyl-1*H*-pyrazole (10p) was synthesized in 81% yield (730 mg) from alkyl bromide **9a** and 3-ethoxyphenol (310 mg, 2.2 mmol) by procedure E and purification by FC: mp 95−97 °C; IR 3080, 3021, 2971, 2925, 1606, 1596, 1552 cm^{-1}; ^1H NMR ($CDCl_3$) δ 7.90 (dd, J = 8.7, J = 2.1, H), 7.51 (dd, J = 8.7, J = 2.1, 2H), 7.39−7.27 (m, 3H), 7.26−7.18 (m, 3H), 6.67 (s, 1H), 6.66−6.54 (m, 3H), 5.17 (s, 2H), 4.03 (q, J = 7.0, 2H), 3.07 (s, 3H), 1.42 (t, J = 7.0, 3H); LC−MS ($APCI^+$) *m/z* 449 (MH^+). Anal. ($C_{25}H_{24}N_2O_4S$) C, H, N.

1-(4-Methanesulfonylphenyl)-3-[(3,4-methylenedioxy)-phenoxymethyl]-5-phenyl-1*H*-pyrazole (10q) was synthesized in 71% yield (640 mg) from alkyl bromide **9a** and 3,4-methylenedioxyphenol (310 mg, 2.2 mmol) by procedure E and purification by FC: mp 98−100 °C; IR 3069, 2923, 1630, 1595, 1551 cm^{-1}; ^1H NMR ($CDCl_3$) δ 7.91 (d, J = 9.0, 2H), 7.52 (d, J = 9.0, 2H), 7.40−7.34 (m, 3H), 7.27−7.24 (m, 2H), 6.74 (d, J = 8.4, 1H), 6.66 (s, 1H), 6.64 (d, J = 2.6, 1H), 6.49 (dd, J = 8.4, J = 2.6, 1H), 5.94 (s, 2H), 5.11 (s, 2H), 3.07 (s, 3H); LC−MS ($APCI^+$) *m/z* 449 (MH^+). Anal. ($C_{24}H_{20}N_2O_5S$) C, H, N.

1-(4-Methanesulfonylphenyl)-3-[(3,5-dimethoxy)phenoxymethyl]-5-phenyl-1*H*-pyrazole (10r) was synthesized in 76% yield (710 mg) from alkyl bromide **9a** and 3,5-dimethoxyphenol (343 mg, 2.2 mmol) by procedure E and purification by FC: mp 120−122 °C; IR 3006, 2969, 2921, 2842, 1600, 1551 cm^{-1}; ^1H NMR ($CDCl_3$) δ 7.90 (d, J = 8.6, 2H), 7.52 (d, J = 8.6, 2H), 7.39−7.35 (m, 3H), 7.27−7.24 (m, 2H), 6.67 (s, 1H), 6.26−6.25 (m, 2H), 6.14 (dd, J = 2.0, J = 2.0, 1H), 5.15 (s, 2H), 3.79 (s, 6H), 3.07 (s, 3H); LC−MS ($APCI^+$) *m/z* 465 (MH^+). Anal. ($C_{25}H_{24}N_2O_5S$) C, H, N.

1-(4-Methanesulfonylphenyl)-3-[(3,4-dimethoxy)phenoxymethyl]-5-phenyl-1*H*-pyrazole (10s) was synthesized in 64% yield (590 mg) from alkyl bromide **9a** and 3,4-dimethoxyphenol (346 mg, 2.2 mmol) by procedure E and purification by FC: mp 118−120 °C; IR 3003, 2934, 2924, 2852, 1594, 1506 cm^{-1}; ^1H NMR ($CDCl_3$) 7.90 (d, J = 8.3, 2H), 7.52 (d, J = 8.3, 2H), 7.39−7.36 (m, 3H), 7.27−7.24 (m, 2H), 6.82 (d, J = 8.6, 1H), 6.68−6.66 (m, 2H), 6.58 (dd, J = 8.9, J = 2.6, 1H), 5.14 (s, 2H), 3.87 (s, 3H), 3.86 (s, 3H), 3.07 (s, 3H); LC−MS ($APCI^+$) *m/z* 465 (MH^+). Anal. ($C_{25}H_{24}N_2O_5S$) C, H, N.

Molecular Modeling. Molecular modeling studies were carried out using INSIGHTII software, version 2000,[39] running on a Silicon graphics workstation. The structure of inhibitors was obtained by means of the BUILDER module and optimized using the CFF91 force field. Docking simulations were performed inside the human COX-2 and 5-LOX enzymes with the automated GOLD program.[40,41] For each inhibitor, the binding mode with the best fit as well as stereoelectronic matching quality was selected. To take into account protein flexibility, all the complexes were then refined with DISCOVER3.[42] The minimization process, using the CVFF force field (dielectric constant 1**r*), includes two steps: the steepest descent algorithm, reaching a convergence of 0.01 kcal mol^{-1} $Å^{-1}$, followed by the conjugated gradient algorithm to reach a final convergence of 0.001 kcal mol^{-1} $Å^{-1}$.

As the 3D structures of human COX-2 and 5-LOX are not yet available in the Protein Data Bank, they were first modeled by homology with murine COX-2 (PDB entry 6COX) and rabbit 15-LOX (PDB entry LOX1), respectively (HOMOLOGY module).[43]

HPLC Analysis of 5-HETE in Whole Blood. Fresh blood was collected in heparinized tubes from normal volunteers. Then, 1 mL aliquots were transferred to heparinized tubes preloaded with either 4 μL of vehicle (DMSO) or 4 μL of test compounds and incubated for 15 min at 37 °C. Then, 40 μM calcium ionophore A 23187 was added. After a final incubation for 15 min at 37 °C, 5-HETE was extracted by ethyl acetate. HPLC analysis was performed on a Hypersil ODS 5 μm column (12.5 mm × 0.48 mm) using a methanol/water/acetic acid 80:20:0.08, pH 6.0, mobile phase at a flow rate of 1 mL/min and UV detection at 234 nm.

In Vitro COX Assay. COX-1 and COX-2 transfected CHO cells were obtained from Innothera Laboratories (Arcueil, France). Cells were seeded into 96-well plates (5.5×10^4 cells/well), and 18 h later, the medium was replaced with fresh medium (Ham's F12 with 10% fetal calf serum) with or without test compounds. After 10 min, cells were stimulated with 20 mmol of arachidonic acid and then for 10 min with the calcium ionophore A 23187. Intracellular PGE_2 was then measured using an enzyme immunoassay system (Amersham Biosciences).

Cell Culture and Cell Proliferation Assay. Human prostate cancer cells were grown at 37 °C in RPMI 1640 medium supplemented with 10% fetal calf serum, in a humidified incubator containing 5% CO_2. In the cell proliferation assay, cells were plated (1.8×10^4 cells/well for PC 3 and 5.0×10^4 cells/well for LNCaP) on 24-well plates. After 3 days, the cell medium was changed to serum-free medium, and the cells were starved for 24 h for culture synchronization. Cells were then incubated in culture medium that contained various concentrations of test compounds, each dissolved in less than 0.1% DMSO. After incubating for 72 h, cell growth was estimated by the colorimetric MTT test.

Cell Cycle Analysis and Apoptosis Detection. Prostate cancer cells LNCaP and PC 3 were seeded into 6-well plate flasks, synchronized for 24 h in serum-free medium, and incubated for 72 h with varying concentrations of test compounds. After incubation, the media were aspirated off and the treated cells were trypsinized for the culture flasks, pooled with the culture supernatants, and centrifuged at 900 rpm. The pelleted cells were resuspended in PBS, fixed by adding cold ethanol (4 °C, overnight), and then incubated for 30 min

in PBS containing RNase and propidium iodide (cell cycle test kit, Becton Dickinson). Cytometric analysis was then performed on a FACScan flow cytometer and the propidium iodide-stained cell populations in the sub-G1 (corresponding to sub-diploid nuclei), G1, S, and G2-M phases were quantified using the Cellquest computer program.

Acknowledgment. This work was completed with the support of research grants to N.P. from the Groupement des Entreprises Françaises dans la Lutte contre le Cancer (GEFLUC Lille-Flandres-Artois) and to C.C. from the Belgian Foundation for Scientific Research (FNRS). The authors thank the Facultés Notre-Dame de la Paix (Namur, Belgium) for the use of the Scientific Computing Facility and Dr. C. Bailly (INSERM U524 and Laboratoire de Pharmacologie Antitumorale du Centre Oscar Lambret, IRCL, Lille, France) for FACS analysis. The technical assistance of A. Lemoine in performing the antiproliferative and proapoptotic assays was also greatly appreciated.

References

(1) Cuendet, M.; Pezzuto, J. M. The role of cyclooxygenase and lipoxygenase in cancer chemoprevention. *Drug Metabol. Drug Interact.* **2000**, *17*, 109−157.
(2) Nie, D.; Honn, K. V. Cyclooxygenase, lipoxygenase and tumor angiogenesis. *Cell Mol. Life Sci.* **2002**, *59*, 799−807.
(3) Gasparini, G.; Longo, R.; Sarmiento, R.; Morabito, A. Inhibitors of cyclo-oxygenase 2: A new class of anticancer agents? *Lancet Oncol.* **2003**, *4*, 605−615.
(4) Haller, D. G. COX-2 inhibitors in oncology. *Semin. Oncol.* **2003**, *30*, 2−8.
(5) Nie, D.; Che, M.; Grignon, D.; Tang, K.; Honn, K. V. Role of eicosanoids in prostate cancer progression. *Cancer Metastasis Rev.* **2001**, *20*, 195−206.
(6) Gupta, S.; Srivastava, M.; Ahmad, N.; Bostwick, D. G.; Mukhtar, H. Over-expression of cyclooxygenase-2 in human prostate adenocarcinoma. *Prostate* **2000**, *42*, 73−78.
(7) Madaan, S.; Abel, P. D.; Chaudhary, K. S.; Heyritt, R.; Stott, M. A.; Stamp, G. W.; Lalani, E. N. Cytoplasmic induction and over-expression of cyclooxygenase-2 in human prostate cancer: Implications for prevention and treatment. *BJU Int.* **2000**, *86*, 736−741.
(8) Hussain, T.; Gupta, S.; Mukhtar, H. Cyclooxygenase-2 and prostate carcinogenesis. *Cancer Lett.* **2003**, *191*, 125−135.
(9) Sabichi, A. L.; Lippman, S. M. COX-2 inhibitors and other NSAIDs in bladder and prostate cancer. *Prog. Exp. Tumor Res.* **2003**, *37*, 163−178.
(10) Attiga, F. A.; Fernandez, P. M.; Weeraratna, A. T.; Manyak, M. J.; Patierno, S. R. Inhibitors of prostaglandin synthesis inhibit human prostate tumor cell invasiveness and reduce the release of matrix metalloproteinases. *Cancer Res.* **2000**, *60*, 4629−4637.
(11) Shureiqi, I.; Lippman, S. M. Lipoxygenase modulation to reverse carcinogenesis. *Cancer Res.* **2001**, *61*, 6307−6312.
(12) Pidgeon, G. P.; Kandouz, M.; Meram, A.; Honn, K. V. Mechanisms controlling cell cycle arrest and induction of apoptosis after 12-lipoxygenase inhibition in prostate cancer cells. *Cancer Res.* **2002**, *62*, 2721−2727.
(13) Hsi, L. C.; Wilson, L. C.; Eling, T. E. Opposing effects of 15-lipoxygenase-1 and −2 metabolites on MAPK signalling in prostate. Alteration in peroxisome proliferators-activated receptor gamma. *J. Biol. Chem.* **2002**, *277*, 40549−40556.
(14) Shappell, S. B.; Gupta, R. A.; Manning, S.; Whitehead, R.; Boeglin, W. E.; Schneider, C.; Case, T.; Price, J.; Jack, G. S.; Wheeler, T. M.; Matusik, R. J.; Brash, A. R.; DuBois, R. N. (15*S*)-hydroxyeicosatetraenoic acid activates peroxisome proliferator-activated receptor γ and inhibits proliferation in PC 3 prostate carcinoma cells. *Cancer Res.* **2001**, *61*, 497−503.
(15) Kelavkar, U. P.; Nixon, J. B.; Cohen, C.; Dillehay, D.; Eling, T. E.; Badr, K. F. Overexpression of 15-lipoxygenase-1 in PC 3 human prostate cancer cells increases tumorigenesis. *Carcinogenesis* **2001**, *22*, 1765−1773.
(16) Anderson, K. M.; Seed, T.; Vos, M.; Mulshine, J.; Meng, J.; Alrefai, W.; Ou, D.; Harris, J. E. 5-lipoxygenase inhibitors reduce PC 3 cell proliferation and initiate non-necrotic cell death. *Prostate* **1998**, *37*, 161−173.
(17) Liu, X. H.; Kirschenbaum, A.; Yao, S.; Lee, R.; Holland, J. F.; Levine, A. C. Inhibition of cyclooxygenase-2 suppresses angiogenesis and the growth of prostate cancer in vivo. *J. Urol.* **2000**, *164*, 820−825.
(18) Song, X.; Lin, H. P.; Johnson, A.; Tseng, P. H.; Yang, Y. T.; Kulp, S. K.; Chen, C. S. Cyclooxygenase-2, player or spectator in cyclooxygenase-2 inhibitor-induced apoptosis in prostate cancer cells. *J. Natl. Cancer Inst.* **2002**, *94*, 585−591.
(19) Zhu, J.; Song, X.; Lin, H. P.; Young, D. C.; Yan, S.; Marquez, V. E.; Chen, C. S. Using cyclooxygenase-2 inhibitors as molecular platforms to develop a new class of apoptosis-inducing agents. *J. Natl. Cancer Inst.* **2002**, *94*, 1745−1757.
(20) Marx, J. Cancer research. Anti-inflammatories inhibit cancer growth—But how? *Science* **2001**, *291*, 581−582.
(21) Srinath, P.; Rao, P. N.; Knaus, E. E.; Suresh, M. R. Effect of cyclooxygenase-2 (COX-2) inhibitors on prostate cancer cell proliferation. *Anticancer Res.* **2003**, *23*, 3923−3928.
(22) Gugliucci, A.; Ranzato, L.; Scorrano, L.; Colonna, R.; Petronilli, V.; Cusan, C.; Prato, M.; Mancini, M.; Pagano, F.; Bernardi, P. Mitochondria are direct targets of the lipoxygenase inhibitor MK886. A strategy for cell killing by combined treatment with MK886 and cyclooxygenase inhibitors. *J. Biol. Chem.* **2002**, *277*, 31789−31795.
(23) Barbey, S.; Goossens, L.; Taverne, T.; Cornet, J.; Choesmel, V.; Rouaud, C.; Gimeno, G.; Yannic-Arnoult, S.; Michaux, C.; Charlier, C.; Houssin, R.; Hénichart, J.-P. Synthesis and activity of a new methoxytetrahydropyran derivative as dual cyclooxygenase-2/5-lipoxygenase inhibitor. *Bioorg. Med. Chem. Lett.* **2002**, *12*, 779−782.
(24) Crawley, G. C.; Dowell, R. I.; Edwards, P. N.; Foster, S.; MacMillan, R. M.; Walker, E. R. H.; Waterson, P. Methoxytetrahydropyrans. A new series of selective and orally potent 5-lipoxygenase inhibitors. *J. Med. Chem.* **1992**, *35*, 2600−2609.
(25) Sajiki, H.; Ong, K. Y. Synthesis of C_2-symmetric (*S*,*S*)-1,4-dibenzyl-DTPA and 1,4-meso-dibenzyl-DTPA via chiral diamines. *Tetrahedron* **1996**, *52*, 14507−14514.
(26) Charlier, C.; Michaux, C. Dual inhibition of cyclooxygenase-2 (COX-2) and 5-lipoxygenase (5-LOX) as a new strategy to provide safer non-steroidal anti-inflammatory drugs. *Eur. J. Med. Chem.* **2003**, *38*, 645−659.
(27) Garavito, R. M.; Malkowski, M. G.; DeWitt, D. L. The structures of prostaglandin endoperoxide H synthases-1 and −2. *Prostaglandins Other Lipid Mediat.* **2002**, *68*−*69*, 129−152.
(28) Kurumbail, R. G.; Stevens, A. M.; Gierse, J. K.; McDonald, J. J.; Stegeman, R. A.; Pak, J. Y.; Gildehaus, D.; Miyashiro, J. M.; Penning, T. D.; Seibert, K.; Isakson, P. C.; Stallings, W. C. Structural basis for selective inhibition of cyclooxygenase-2 by anti-inflammatory agents. *Nature* **1996**, *384*, 644−648.
(29) Rowlinson, S. W.; Kiefer, J. R.; Prusakiewicz, J. J.; Pawlitz, J. L.; Kozak, K. R.; Kalgutkar, A. S.; Stallings, W. C.; Kurumbail, R. G.; Marnett, L. J. A novel mechanism of cyclooxygenase-2 inhibition involving interactions with Ser-530 and Tyr-385. *J. Biol. Chem.* **2003**, *278*, 45763−45769.
(30) Goodford, P. J. A computational procedure for determining energetically favorable binding sites on biologically important macromolecules. *J. Med. Chem.* **1985**, *28*, 849−857.
(31) Kazanov, D.; Dvory-Sobol, H.; Pick, M.; Liberman, E.; Strier, L.; Choen-Noyman, E.; Deutsch, V.; Kunik, T.; Arber, N. Celecoxib but not rofecoxib inhibits the growth of transformed cells in vitro. *Clin. Cancer Res.* **2004**, *10*, 267−271.
(32) Grosch, S.; Tegeder, I.; Niederberger, E.; Brautigam, L.; Geisslinger, G. COX-2 independent induction of cell cycle arrest and apoptosis in colon cancer cells by the selective COX-2 inhibitor celecoxib. *FASEB J.* **2001**, *15*, 2742−2744.
(33) Kundu, N.; Smyth, M. J.; Samsel, L.; Fulton, A. M. Cyclooxygenase inhibitors block cell growth, increase ceramide and inhibit cell cycle. *Breast Cancer Res. Treat.* **2002**, *76*, 57−64.
(34) Seelan, R. S.; Qian, C.; Yokomizo, A.; Bostwick, D. G.; Smith, D. I.; Liu, W. Human acid ceramidase is overexpressed but not mutated in prostate cancer. *Genes Chromosomes Cancer* **2000**, *29*, 137−146.
(35) Mimeault, M.; Pommery, N.; Wattez, N.; Bailly, C.; Hénichart, J.-P. Anti-proliferative and apoptotic effects of anandamide in human prostatic cancer cell lines: Implication of epidermal growth factor receptor down-regulation and ceramide production. *Prostate* **2003**, *56*, 1−12.
(36) Zha, S.; Gage, W. R.; Sauvageot, J.; Saria, E. A.; Putzi, M. J.; Ewing, C. M.; Faith, D. A.; Nelson, W. G.; De Marzo, A. M.; Isaacs, W. B. Cyclooxygenase-2 is upregulated in proliferative inflammatory atrophy of the prostate but not in prostate carcinoma. *Cancer Res.* **2001**, *61*, 8617−8623.
(37) Weis, C. D. Ger. Offen. 2,827,062, 1979; *Chem. Abstr.* **1979**, *90*, 151814c.
(38) Brecker, L.; Pogorevc, H.; Griengl, H.; Steiner, W.; Kappe, T.; Ribbons, D. W. Synthesis of 2,4-diketo acids and their aqueous solution structures. *New J. Chem.* **1999**, *23*, 437−446.
(39) *InsightII*; version 2000; Accelrys Inc.: San Diego, CA.

(40) Jones, G.; Willett, P.; Glen, R. C. Molecular recognition of receptor sites using a genetic algorithm with a description of desolvation. *J. Mol. Biol.* **1995**, *245*, 43−53.
(41) Jones, G.; Willett, P.; Glen, R. C.; Leach, A. R.; Taylor, R. Development and validation of a genetic algorithm for flexible docking. *J. Mol. Biol.* **1997**, *267*, 727−748.
(42) *Discover, Force field Simulations, User guide*, Part 1; Biosym/MSI: San Diego, CA, 1996.
(43) *Homology, User guide*; Biosym/MSI: San Diego, CA, 1993.

JM0407761